*American Journal of Energy Engineering*
2024, Vol. 12, No. 4, pp. 80-93
https://doi.org/10.11648/j.ajee.20241204.11

Research Article

# Validity of Laws for Predicting Lifespan of Welded Points Under Variable Loading

**Bianzeube Tikri[1], Djonglibet Wel-Doret[1, *], Dougabka Dao[2]**

[1]Department of Technical Sciences, University of N'Djamena, N'Djamena, Chad
[2]Department of Mechanical Engineering, Polytechnic University, Mongo, Chad

## Abstract

The article examines the validity of the laws for predicting the life of welded points under variable amplitude loading, using three steels (HE360D, XE360D and XES) supplied by ArcelorMittal to Renault for the manufacture of automobile chassis parts. The fatigue tests revealed two modes of failure: cracking of the sheets at medium stresses and shearing of the molten core at high forces. For lifespan prediction, three damage laws were studied: Miner's law, Mesmacque and Amrouche law, and a proposed model. Miner's law, despite its simplicity and wide distribution, shows notable limitations in the presence of variable loads, because it does not take into account the interactions between successive load levels. The law of Mesmacque and Amrouche uses a damage indicator linked to the FN curve of the material, allowing a cycle by cycle estimation of the residual lifespan. However, it remains non-conservative at low effort. The proposed model, based on Chaboche law, overcomes some of its theoretical drawbacks, notably the dependence on the calibration parameters of the SN curve. By fitting this curve within a specific calibration window, the model improves forecast accuracy by taking into account parameter variability. This proposed model provides more reliable lifespan predictions that better correlate with experimental results, especially for low effort levels where Miner's law fails. The validation approach is based on comparing the predictions of the damage laws with the experimental results, by evaluating the deviation from the first bisector of the graphs. The results show that Miner's law is unsuitable for effort levels, while the proposed model turns out to be the most precise and conservative. The law of Mesmacque and Amrouche falls between the two, presenting a certain justice but remaining overall non-conservative. In conclusion, the proposed model offers a better match with experimental data, making its predictions more reliable for industrial applications.

## Keywords

Materials Tested, Modes of Failure, Fatigue Tests, Damage Laws, Lifespan Prediction, Validation of Laws

## 1. Introduction

The objective of this research is to compare the fatigue damage laws with the real behavior of welded points subjected to stresses of variable amplitude. The first part consists of a presentation of the damage laws used in this study. The emphasis is placed on the formalism of the new lifespan calculation law proposed to the laboratory, and whose basic principle is analogous to that of Chaboche law [1, 2]. It relates to the non-linear nature of the fatigue damage function

*Corresponding author: djonglibetamadin@yahoo.fr (Djonglibet Wel-Doret)

**Received:** 25 September 2024; **Accepted:** 15 October 2024; **Published:** 11 November 2024

and its accumulation, to the effect of the order of application of the stress cycles (also called sequence effect), to the taking into account of the stress average, and finally and above all to the determination of the main parameters of the law, that is to say to the identification of its parameters from the basic properties of the material in fatigue (S-N curve). This last point constitutes the particularity of the proposed model, the integration of the damage under constant amplitude making it possible to find the expression of the S-N curve of the material, which was not the case with the Chaboche model [1, 3]. A notable point is the necessary transformation of the formalism of damage laws usually translated in terms of stresses, into laws expressed here in efforts to respond to the experimental characterization of the fatigue resistance of welded points under load ratio equal to 0, 1. The rest of this article is devoted to the comparison with the experimental results and the discussion of the predictions of the laws of Miner, of Mesmacque and Amrouche and of that proposed, for the three materials and the two types of stress of variable amplitude (overloads of ratios 1, 4 and 2, 3).

## 2. Materials Tested

Three distinct steels named HE360D, XE360D and XES were used for this experimental campaign. These steels are produced by ArcelorMittal in the form of hot-rolled sheets and are delivered to the automobile manufacturer Renault for the manufacture of automobile chassis and/or ground connection parts. The thickness of the sheets of the HE360D steel studied is 2, 5 mm while that of the sheets of the other two steels is 1, 2 mm. All the test pieces used for this experimental campaign were made from the sheets as delivered and with welder settings corresponding to industrial practice [4-6]. The static mechanical strength of the welded assemblies was established through monotonic tensile tests carried out until failure on each type of specimen. Table 1 summarizes the maximum tensile force obtained for each material during these monotonic tensile tests.

***Table 1.*** *Maximum tensile force of spot welded specimens.*

| Material | HE 360D | XE 360D | XES |
|---|---|---|---|
| Maximum effort | 24270 N | 12540 N | 9480 N |

## 3. Modes of Fatigue Failure of Specimens

Two modes of failure of the specimens are observed during the tests carried out until rupture. The first mode results in cracking of the sheets in the part transmitting the tensile force to the molten core connecting the two sheets; the second mode is shearing of the molten core in the plane common to the two sheets. Figure 1 shows two test pieces broken according to the two distinct modes of failure: (a) by complete cracking and rupture of one of the two sheets, (b) by rupture of the molten core of the welded point in its minimum cross section.

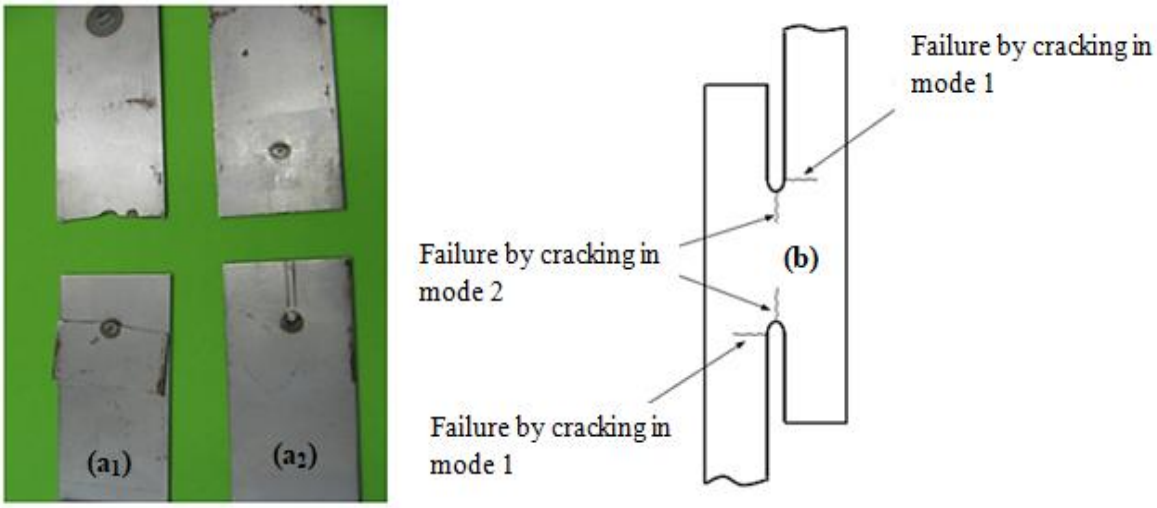


***Figure 1.*** *Failure by cracking (a1), failure by shearing (a2), and the experimental sites of initiation and cracking of the specimen (b).*
*Preferred field*

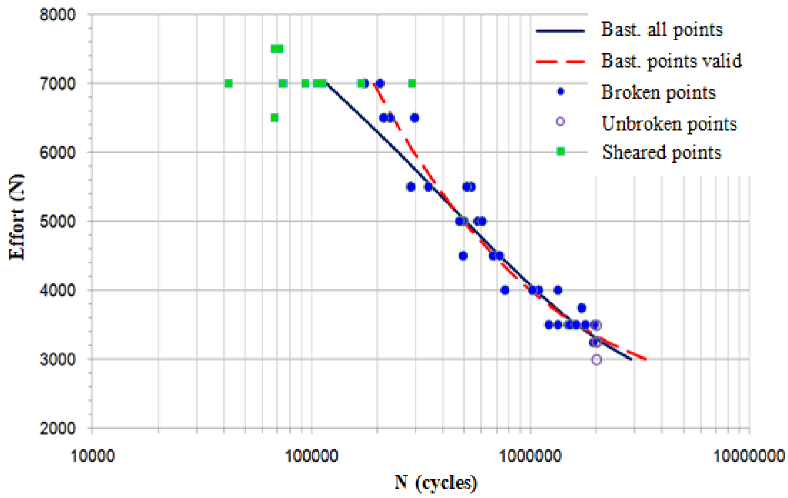


***Figure 2.*** *Preferred domain of the two modes of fatigue failure of spot-welded HE360D steel specimens according to the loading level.*

## 4. Damage Laws Used for Lifespan Prediction

Predicting the fatigue life of structures under variable amplitude stress is a necessity in the field of automobile manufacturing because, to be competitive, the solution must be optimized as closely as possible in order to meet ever more demanding specifications. The progressive degradation of the properties of materials, linked to the application of variable forces over time, the repetition of which can lead to breakage by cracking of the part or structure, has today become an essential concern in any approach to sizing. The hazards of the road (potholes, sidewalks, cobblestones, etc.) on which the vehicle rolls give rise to occasional overloads on the chassis elements assembled by means of spot welding. These overloads, generated by deterioration in road conditions and the way the vehicle is driven, are likely to have a significant influence on the lifespan of the sheets bonded by welding [7].

To improve structures from the point of view of fatigue resistance, the design office must equip itself with sizing tools allowing it to predict, during design, their fatigue behavior under variable loading and thus reduce the costs and delays in the stages of prototype development. Among the fatigue design tools are the laws of damage and accumulation of damage which are put to the test here on the welded points stressed in tension-shear. This paragraph presents, on the basis of work carried out in the laboratory and relating to nonlinear damage laws [8], a fatigue damage law proposed when the F-N curve of the material is described by the Basquin model. This proposes formalism close to that of Chaboche with regard to the effect of the order of appearance of the stress cycles, the influence of the average stress and the non-linear nature of the accumulation of damage. Two other laws are also used, that of Mesmacque and Amrouche as well as that of Miner [9, 10]. Miner's law is linear, the other two are non-linear and cumulative damage is also non-linear. The damage laws make it possible, in general, once the lifespan of the material relative to each extracted cycle has been determined, to calculate the corresponding damage and add it up. This cumulative damage leads to the estimation of the lifespan of the material in terms of the number of cycles at the initiation of a macroscopic crack. Three damage laws expressed in forces are tested against the results of fatigue tests with overload carried out as part of this work.

### 4.1. Miner Law

The lifespan of the material is defined by the number of cycles at the initiation of a crack (or rupture) $N_R$. Thus, the application of n cycles ($n < N_R$) results in partial deterioration or damage of the material. Knowledge of this damage is important because it makes it possible to evaluate the residual lifespan and to decide whether or not to replace the component to avoid fatigue damage.

The simplest rule for evaluating the degradation of the fatigue resistance capabilities of the material consists of considering a linear evolution of the damage. It stipulates that the damage suffered by the material at each cycle is a function of the level of effort representative of this cycle. For n cycles applied, the quantity is called damage [10]:

$$D = \sum_{i=1}^{k} d_i = \sum_i \frac{n_i}{N_i} \quad (1)$$

where: ni is the number of applied cycles identical to that considered,

Ni is the number of cycles supported by the material at the initiation of a crack.

According to this concept, the initiation of a crack appears in theory when the damage D is equal to unity.

Simple and very widely used, this method of predicting lifespan according to Miner presents proven and recognized defects in the presence of "low-high" and "high-low" type loadings, that is to say loadings at increasing or decreasing loading amplitude respectively. Miner's law ignores the interactions, from a fatigue point of view, between the different successive loading levels. What is more, the forecast error generated by Miner's law is approximately of the same order but with opposite trends for these two types of "extreme" loading, with monotonous variation in amplitude. When these two trends are encountered during the same loading history, the successive forecast errors partially compensate for each other. This explains the success still encountered today by this law of fatigue damage of variable amplitude.

## 4.2. Mesmacque and Amrouche Law

The law of Mesmacque and Amrouche is based on a damage indicator linked cycle after cycle to the F-N curve of the material. This indicator, called damaged effort, corresponds to the instantaneous residual life [9]:

$$D_i = \frac{F_{ied} - F_i}{F_u - F_i} \tag{2}$$

Where: $F_{ied}$ is the damaged effort,

$F_i$ and Fu are respectively the force applied at level i and the ultimate force of the material,

$D_i$ is the damage variable.

When D is equal to unity, the material reaches its maximum damage level, which corresponds to the initiation of a crack.

## 4.3. Law Proposed to the Laboratory

*a) Justification for the modification of Chaboche law*

The disadvantage of Chaboche law lies in the differences in lifespans that we obtain for a given material, depending on the calibration domain used, when its S-N curve, transferred into Chaboche space, is assimilated to a straight line (figure 3) [11]. The lifespan prediction by this law is therefore dependent on the calibration domain used (figure 4).

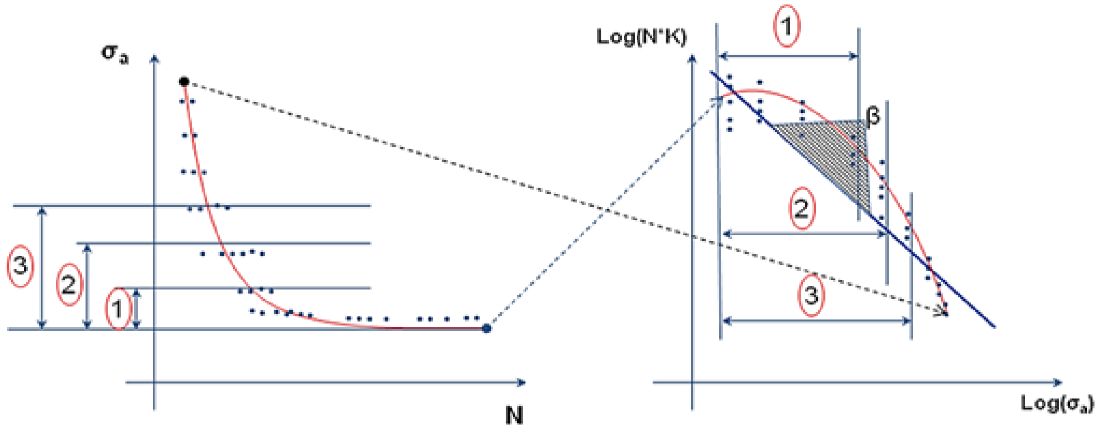


***Figure 3.*** *Principle of calibration of Chaboche law.*

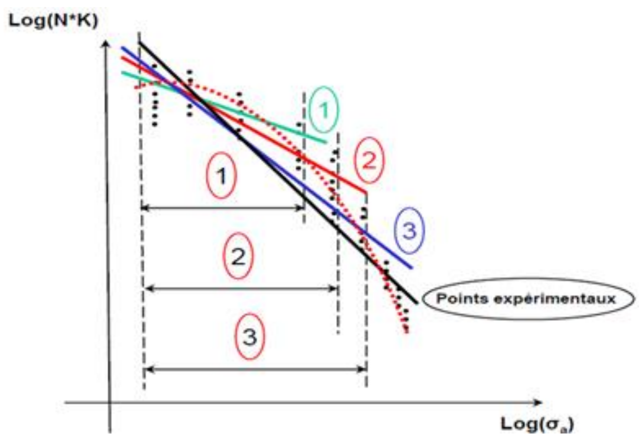


***Figure 4.*** *Sensitivity of the calibration of Chaboche law to the window used of the S-N curve.*

To try to remedy this drawback of Chaboche's law, a new law was proposed to achieve the accumulation of fatigue damage under loading of variable amplitude. The formalism of the law essentially has the characteristic of restoring the expression of the S-N curve specific to the material when the integration of the damage is carried out under a loading of constant amplitude. This is how a particular formalism was proposed for each type of classic S-N curve: Wöhler, Basquin, Stromeyer or Bastenaire models [8].

*b) Transformation into effort of the proposed model, based on Basquin's F-N curve*

The principle of the proposed model is a differential form of fatigue damage whose integration under constant amplitude loading leads to the F-N curve modeled by Basquin. For reasons of difficulty in defining a representative stress level within the welded point itself or in the sheets assembled in the vicinity of the welded point, we linked the damage variable to the maximum force of the cycle applied to the specimen. The damage is thus established using the force cycle (distinguishing the average part of the amplitude).

*c) Differential expression of the law*

The general expression which reflects the evolution of fatigue damage is expressed in differential form by:

$$\delta D = \left[1 - (1 - D)^{\beta+1}\right]^{\alpha(F_{max},F_D,F_u)} \cdot \left[\frac{F_u - F_D}{F_{max} - F_C} \cdot \left(\frac{F_{max}}{\sqrt{M_0\left(1-\frac{0.55 \cdot F_{max}}{A \cdot F_u}\right) \cdot (1 - D)}}\right)^{\beta}\right] \delta N \quad (3)$$

Where:

$\delta D$ is the increase in damage D of the material, due to $\delta N$ identical cycle(s),

$F_u$ is the maximum tensile breaking strength of the specimen,

$F_C$ is the conventional endurance limit at $2.10^6$ cycles,

$F_D$ is the endurance limit determined by smoothing the experimental points of the F-N curve using the ESOPE software,

The coefficient α, function of the maximum effort $F_{max}$, the conventional endurance limit $F_C$, the endurance limits $F_D$ and the maximum tensile resistance Fu, reflects the non-linearity of the accumulation of damage; it is defined by:

$$\alpha = 1 - a\left\langle\frac{F_{max} - F_C}{F_u - F_D}\right\rangle \quad (4)$$

a, A, β and $M_o$ are coefficients specific to the material.

*d) Integration of the proposed damage law*

The accumulation of damage is carried out step by step for all the cycles encountered during loading. The lifespan of the material is established by integration of the differential damage law written in the form:

$$\frac{(1 - D)^{\beta}}{\left[1 - (1 - D)^{\beta+1}\right]^{\alpha}} \cdot \delta D = \left[\frac{F_u - F_D}{F_{max} - F_C} \cdot \left(\frac{F_{max}}{\sqrt{M_0\left(1-\frac{0.55 \cdot F_{max}}{A \cdot F_u}\right)}}\right)^{\beta}\right] \delta N \quad (5)$$

$$\Leftrightarrow N_{fj} = \frac{1}{aM_0^{-0.5\beta} \cdot (1 + \beta)} \cdot \left(\frac{F_{max}}{\sqrt{\left(1-\frac{0.55 \cdot F_{max}}{A \cdot F_u}\right)}}\right)^{-\beta} \quad (6)$$

$N_{fj}$ is the number of cycles necessary for the initiation of a crack within the material under a loading of constant amplitude described by the maximum force cycle Fmaxi. It is therefore an expression of the F-N curve of the material. The identification of this expression with the F-N curve intrinsic to the spot-welded specimens therefore makes it possible to determine the coefficients of the proposed damage law.

*e) Identification of model parameters*

The application of this new damage law, like other laws used elsewhere, requires knowledge of the F-N curve of the material. The analytical expression of the F-N curve used for this application is that of Basquin (this is the choice of the car manufacturer). For each of the three steel grades studied (HE 360 D, XE 360 D, The ESOPE software then made it possible to establish the coefficients of the Basquin model which smoothes and describes all the experimental results of the established F-N curve. The proposed damage law itself leads, under constant amplitude, to an equation of the F-N curve identical to that of Basquin; the identification in practice of the material coefficients is done by term-by-term comparison of the experimental Basquin curve and that induced by the law. Table 2. brings together the values thus obtained for the parameters for each of the three steels studied.

***Table 2.*** *Parameters of the damage law proposed for the three steel grades studied.*

| Parameter | Steels grades | | |
|---|---|---|---|
| | **HE 360D** | **XE 360D** | **XES** |
| B | 0,3194 | 0,2761 | 0,1306 |
| $aM_0^{-0.5\beta}$ | 0,2336 | 0,2782 | 0,5021 |

## 5. Estimated Lifespan of Spot-Welded Specimens Under Variable Amplitude Loading

The regular incidental overloads to which the spot-welded specimens are subjected in fact lead to a loading of variable amplitude. This is particular since only two distinct cycles constitute the applied loading (the so-called "basic" cycle and the overload cycle which is applied regularly). The objective of the work carried out and presented in this paragraph is therefore to study the effectiveness of the damage laws presented in the previous paragraph through their ability to predict the evolution of the fatigue behavior of spot welded specimens subjected to the different types of overloads.

### 5.1. Damage Laws Validation Approach

The validity of a damage law is measured by the relative difference between its prediction and the experimental results which serve as a "judge of the peace". Taking into account the order of appearance of the cycles (sequence effect), the average part of the cycles, the non-linear evolution of the damage are all points which, on a theoretical level, help to bring the forecasts closer together. of the model of the observed experimental trends. Quantitatively, it is the relative difference in the lifespans obtained which materializes the accuracy of the law. We therefore use the following criterion to establish the prediction error of a damage model with regard to the lifespan obtained experimentally:

$$ERP = \left(\frac{N_{exp} - N_{mod}}{N_{exp}}\right) x100 \quad (7)$$

Where: $N_{exp}$ is the experimental lifespan,
$N_{mod}$ is the lifespan provided for by the damage law.
The interpretation of the ERP error index is as follows:

1) if ERP ≥ 0, the forecast is conservative and places the designer "safe" (since the calculated lifespan is lower than that obtained experimentally).
2) if ERP < 0, the forecast is non-conservative, the lifespan forecast from the model is greater than that obtained experimentally.

In what follows we evaluate the quality or relevance of the three damage laws studied (Miner, Mesmacque and Amrouche, and the proposed model) for each of the three materials tested experimentally and with the two overload ratios 1, 4 and 2, 3.

The dispersion of fatigue test results leads to very variable lifespans for the same level of effort, while the prediction of lifespan by a damage law is based on the data of the F-N curve, estimated for a survival probability of 50% by the ESOPE software. Comparing the lifespan estimated by a damage law at a given effort level with all the experimental results obtained for this loading level would lead to masking the accuracy "in deterministic prediction" of the law by the dispersion of the experimental lifespan inherent to the fatigue phenomenon. Consequently, to have a clearer vision of the validity of the damage laws, the experimental curve smoothed by the ESOPE software is compared with the curves corresponding to the lifespan predictions for each of the laws of Miner, Mesmacque and Amrouche and of that proposed in the laboratory. This is therefore the comparison of Gassner curves where the total number of cycles applied to the initiation of a crack appear on the abscissa and on the ordinate, the level representative of the loading, that is to say the force maximum corresponding to the basic cycles of this loading. The superposition of the four Gassner curves within a graph thus makes it possible to establish by comparison the respective validity of each model.

For a more quantitative relative comparison of real and estimated lifespans, the ERP error index is calculated, for each law, for several values of the maximum effort of the basic cycles. A table groups the values obtained for each pair (material, overload ratio) and a histogram provides graphic support for these different calculations.

### 5.2. Presentation of the Results of the Damage Laws for Each Material and Each Type of Overload

All six material-loading pairs of variable amplitude tested experimentally serve as the basis for a validity test of the three damage laws studied. The experimental Gassner curve is plotted on a graph where the predictions of the three laws studied are also plotted. For several particular values of the maximum force of the basic cycle (from 3500 N to 6000 N in general with a step of 500 N), the experimental lifespan (from the smoothing of the experimental points given by the ESOPE software) is compared to the lifespans given by the three damage laws used. A table brings together the lifespans obtained (expressed in cycles) for each value representative of the loading (expressed in N). A histogram gives a Cartesian scale representation of the lifespan forecast errors specific to each law.

For each material-overload ratio pair are therefore given successively:

1) the Gassner curves following the three damage models studied as well as the experimental Gassner curve,
2) a summary table of the experimental and calculated lifespans for several loading values corresponding to the basic cycles,
3) a histogram showing the relative forecast errors (ERP) of the three models.

Material HE 360 D – Overload ratio: 1, 4

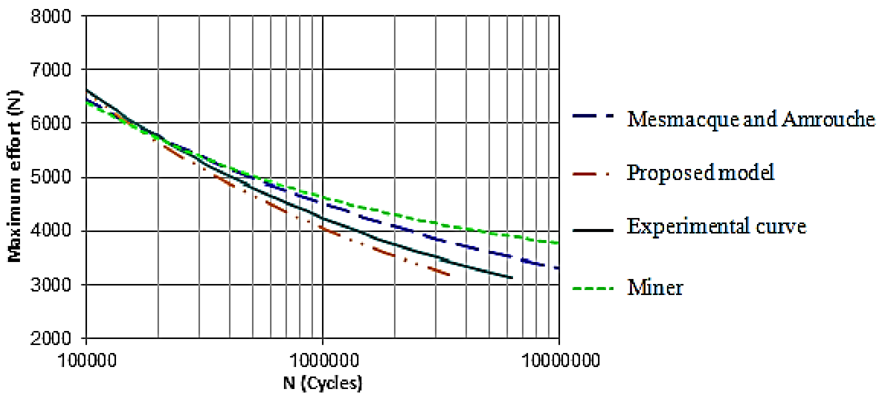


*Figure 5. HE 360 D material, ratio 1.4 overloads: Gassner curves.*

***Table 3.*** *Material HE 360 D, ratio overloads 1.4: prediction errors of damage laws.*

| Maximum effort of the basic cycle | Experimental lifespan | Miner | | Mesmacque and Amrouche | | Proposed model | |
|---|---|---|---|---|---|---|---|
| | | lifespan | ERP (%) | lifespan | ERP (%) | lifespan | ERP (%) |
| 3500 | 3 032 400 | 36 800 000 | -1113,6 | 6 393 400 | -110,8 | 2 196 600 | 27,6 |
| 4000 | 1 422 100 | 4 525 300 | -218,2 | 2 323 400 | -63,4 | 1 085 200 | 23,7 |
| 4500 | 727 600 | 1 378 500 | -89,5 | 1 007 800 | -38,5 | 586 000 | 19,5 |
| 5000 | 409 600 | 539 100 | -31,6 | 495 000 | -20,8 | 368 500 | 10,0 |
| 5500 | 261 800 | 272 900 | -4,2 | 276 500 | -5,6 | 244 700 | 6,5 |
| 6000 | 176 200 | 159 400 | 9,5 | 164 000 | 6,9 | 171 200 | 2,8 |

The prediction error of Miner's law for a maximum effort of the base cycle equal to 3500 N is so large that this loading case does not appear in the representation histogram in figure 7. The errors in the other cases being significantly smaller, they would be disproportionate and therefore difficult to read.

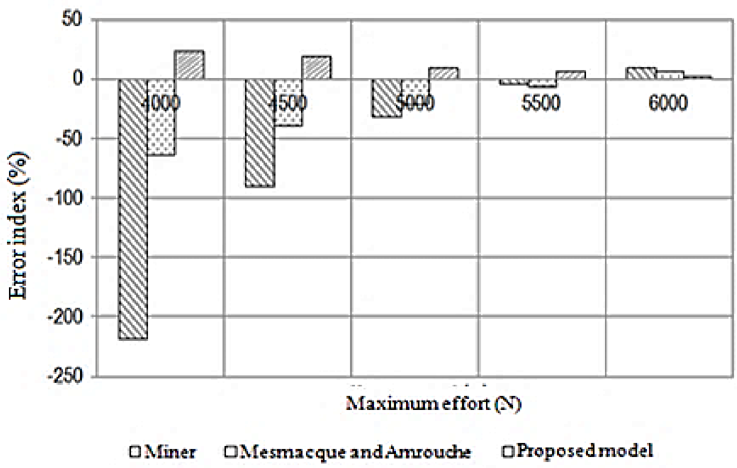


***Figure 6.*** *Material HE 360 D overloads of ratio 1, 4: representation of the prediction errors of the damage laws.*

The proposed model is the only one to be consistently conservative among the three lifespan prediction models studied; Miner's law and that of Mesmacque and Amrouche are non-conservative except for high loading levels. The lifespan prediction differences are much greater for low loading levels than for high levels; there is even a convergence of model predictions and the experimental curve towards a loading level equal to 5800 N. Miner's model is very far, from the point of view of calculated lifespans, from the real behavior of the specimens welded by point for low effort loading.

Material HE 360 D – Overload ratio: 2, 3

***Table 4.*** *Material HE 360 D, ratio overloads 2, 3: prediction errors of damage laws.*

| Maximum effort of the basic cycle | Experimental lifespan | Miner | | Mesmacque and Amrouche | | Proposed model | |
|---|---|---|---|---|---|---|---|
| | | lifespan | ERP (%) | lifespan | ERP (%) | lifespan | ERP (%) |
| 3500 | 3 008 600 | 19 882 500 | -560,8 | 4 895 400 | -62,7 | 2 166 600 | 27,5 |
| 4000 | 1 431 900 | 3 016 800 | -110,7 | 1 988 300 | -38,9 | 1 248 500 | 12,8 |

| Maximum effort of the basic cycle | Experimental lifespan | Miner | | Mesmacque and Amrouche | | Proposed model | |
|---|---|---|---|---|---|---|---|
| | | lifespan | ERP (%) | lifespan | ERP (%) | lifespan | ERP (%) |
| 4500 | 718 600 | 974 600 | -35,6 | 867 100 | -20,7 | 643 700 | 10,4 |
| 5000 | 410 600 | 415 800 | -1,3 | 447 800 | -9,1 | 385 800 | 6,0 |
| 5500 | 251 800 | 213 700 | 15,1 | 245 700 | 2,4 | 244 700 | 2,8 |
| 6000 | 177 200 | 120 800 | 31,8 | 149 600 | 15,6 | 176 600 | 0,3 |

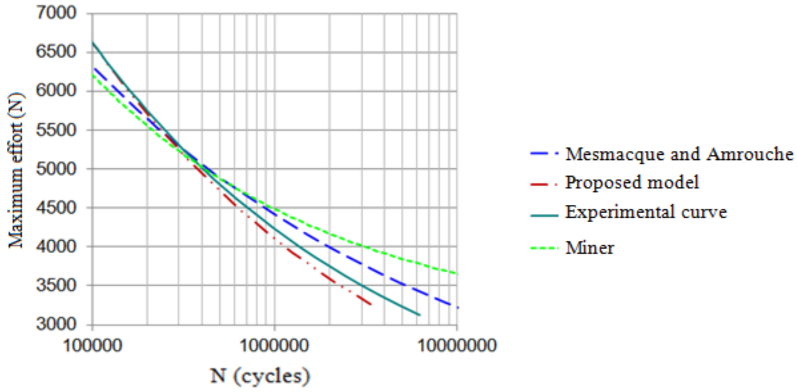


***Figure 7.*** *Material HE 360 D overloads of ratio 2, 3: Gassner curves.*

As previously, the case of the maximum force of 3500 N for the basic cycle is not transcribed in the histogram which follows, due to the too great disproportion observed in this case for the prediction of Miner's law.

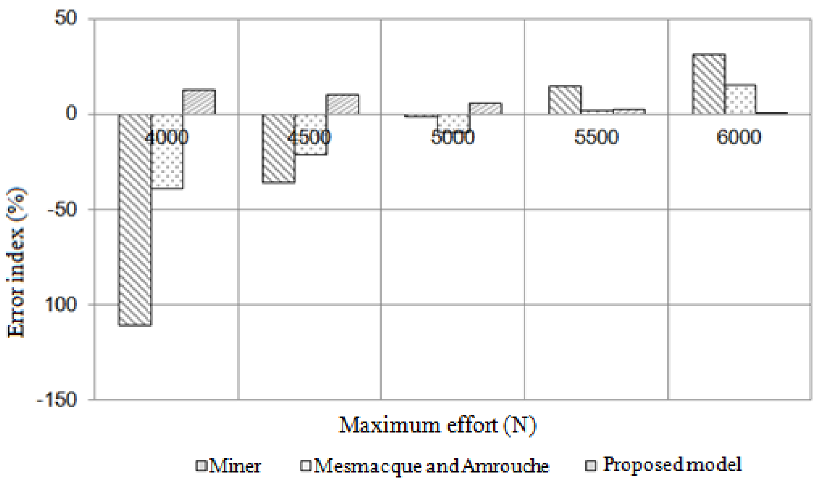


***Figure 8.*** *Material HE 360D, overloads of ratio 2, 3: representation of prediction errors of damage laws.*

The observations of the comparison of lifespan predictions – actual lifespans are quite similar for this overload ratio of 2, 3 as for the overload ratio of 1, 4:

1) the proposed model is the only one to always be conservative compared to the experimental Gassner curve,
2) Miner's law and the Mesmacque and Amrouche model are non-conservative at low loading levels and conservative at high effort levels,
3) the convergence of the three models and the experimental curve is observed at a slightly lower level than in the previous case, that is to say around 5300 N.
4) the predictions given by Miner's law are very far from

reality for low loading levels.

Material XE 360 D – Overload ratio: 1.4

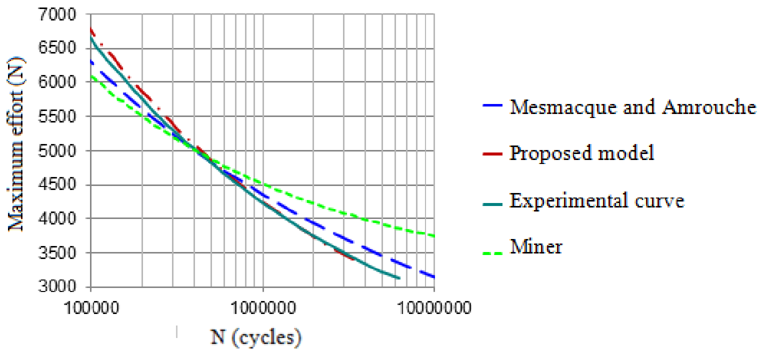


*Figure 9. Material XE 360 D, overloads of ratio 1.4: Gassner curves.*

*Table 5. Material XE 360 D, ratio overloads 1.4: prediction errors of damage laws.*

| Maximum effort of the basic cycle | Experimental lifespan | Miner | | Mesmacque and Amrouche | | Proposed model | |
|---|---|---|---|---|---|---|---|
| | | lifespan | ERP (%) | lifespan | ERP (%) | lifespan | ERP (%) |
| 3500 | 3 033 400 | 35 700 300 | -1076,9 | 4 682 100 | -54,3 | 2 998 900 | 1,1 |
| 4000 | 1 430 100 | 3 965 600 | -177,3 | 1 836 600 | -28,4 | 1 426 500 | 0,3 |
| 4500 | 731 900 | 1 098 600 | -50,1 | 822 000 | -12,3 | 733 000 | -0,2 |
| 5000 | 413 600 | 412 500 | 0,3 | 408 800 | 1,2 | 423 600 | -2,4 |
| 5500 | 252 800 | 197 700 | 21,8 | 233 700 | 7,6 | 261 100 | -3,3 |
| 6000 | 172 000 | 117 800 | 31,5 | 139 600 | 18,8 | 182 100 | -5,9 |

As for the HE 360 D material, the case of the maximum force of the basic cycle equal to 3500 N is not indicated in the histogram which follows for a reason of disproportion of the life expectancy by the law of Mine in this case.

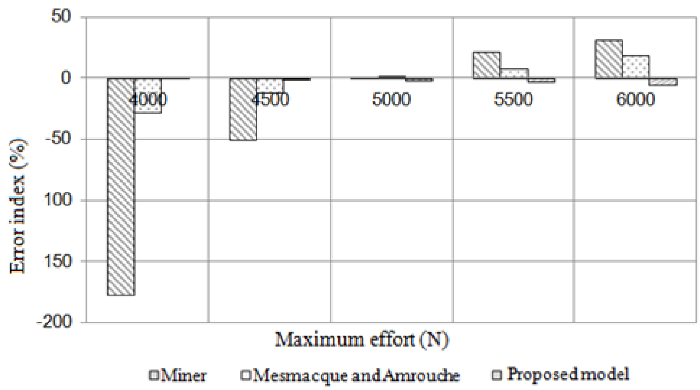


*Figure 10. Material XE 360 D, ratio overloads 1, 4: representation of prediction errors of damage laws.*

For this second material with the overload ratio of 1, 4, Miner's law leads to lifespan predictions very far from the experimental lifespans for low loading levels. On the contrary, the proposed law gives forecasts that are particularly well correlated with experimentation, slightly conservative at a low level of effort and slightly non-conservative at a higher level. The law of Mesmacque and Amrouche and that of Miner present an opposite trend (non-conservative at low level and conservative at high level of effort).

The damage models all three converge significantly towards the experimental lifespans for a maximum value of the basic cycle force of around 4800 N.

Material XE 360 D – Overload ratio: 2, 3

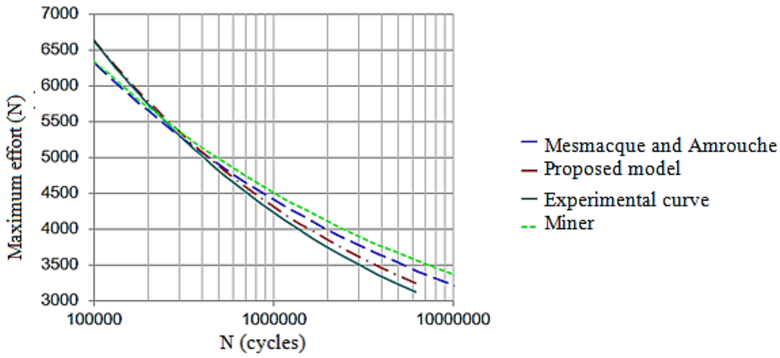


***Figure 11***. *Material XE 360 D, overloads of ratio 2, 3: Gassner curves.*

***Table 6***. *Material XE 360 D, ratio overload 2, 3: prediction errors of damage laws.*

| Maximum effort of the basic cycle | Experimental lifespan | Miner | | Mesmacque and Amrouche | | Proposed model | |
|---|---|---|---|---|---|---|---|
| | | lifespan | ERP (%) | lifespan | ERP (%) | lifespan | ERP (%) |
| 3500 | 3 037 000 | 6 443 900 | -102,3 | 4 752 800 | -56,5 | 3 462 700 | -23,3 |
| 4000 | 1 469 100 | 2 427 400 | -65,2 | 1 929 600 | -31,3 | 1 718 900 | -17,0 |
| 4500 | 708 700 | 1 065 200 | -50,3 | 862 000 | -21,6 | 770 600 | -8,7 |
| 5000 | 413 600 | 484 600 | -17,2 | 439 800 | -6,3 | 423 500 | -2,4 |
| 5500 | 258800 | 247 500 | 4,4 | 245 000 | 5,3 | 263 200 | -1,7 |
| 6000 | 178200 | 152 200 | 14,6 | 149 700 | 16,0 | 179 700 | -0,8 |

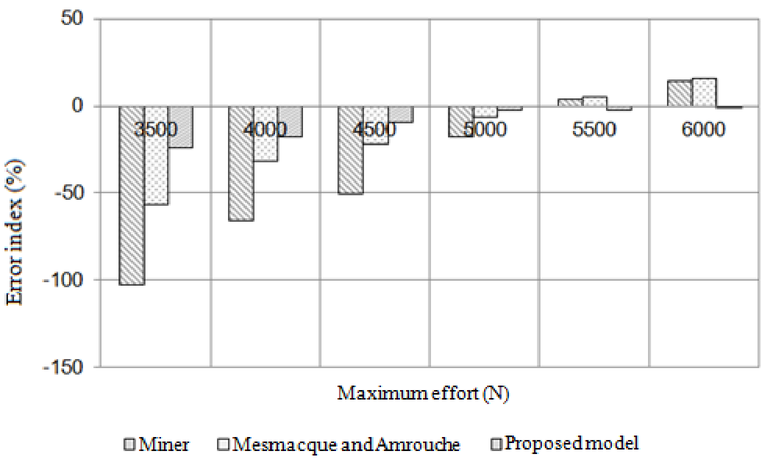


***Figure 12***. *Material XE 360 D, overloads of ratio 2, 3: representation of prediction errors of damage laws.*

For the three damage laws, the largest relative differences are observed for the lowest loading levels. Miner's law gives lifespan predictions that are furthest from actual lifespans. The laws of Miner and of Mesmacque and Amrouche are non-conservative at low effort levels and conservative at higher levels while the proposed law is non-conservative whatever the level of effort analyzed. The difference observed with the actual lifespans is, as for the overload ratio of 1, 4, particularly small for the proposed model. The convergence of all the models and experimental lifetimes is observed for a force level of around 5300 N.

The predictions of the three damage laws are generally quite satisfactory over all tested levels of the experimental Gassner curve. Miner's law is this time systematically conservative and is particularly in agreement with the experimental lifetimes for high levels of effort. The two other laws tested are non-conservative at low level of effort and conservative at high level. The convergence of the models studied and the experimental curve takes place here for a maximum value of the effort of the basic cycles of the order of 5300N.

## 6. Respective Validity of the Damage Laws Used

A perhaps even more explicit description of the validity of the damage laws which were used to establish the lifespan of spot-welded specimens under variable amplitude loading consists of representing the lifespans obtained experimentally as a function of those calculated. For each material-overload ratio pair, the lack of validity of a law is measured by the distance of the curve obtained from the first bisector of the graph thus established. When the characteristic obtained is to the right of the first bisector of the graph, find them to the left of this bisector. Figures 13 to 18 give these representations for the three materials HE 360 D, XE 360 D and XES successively and, for each of them, for the two overload ratios 1, 4 and 2, 3.

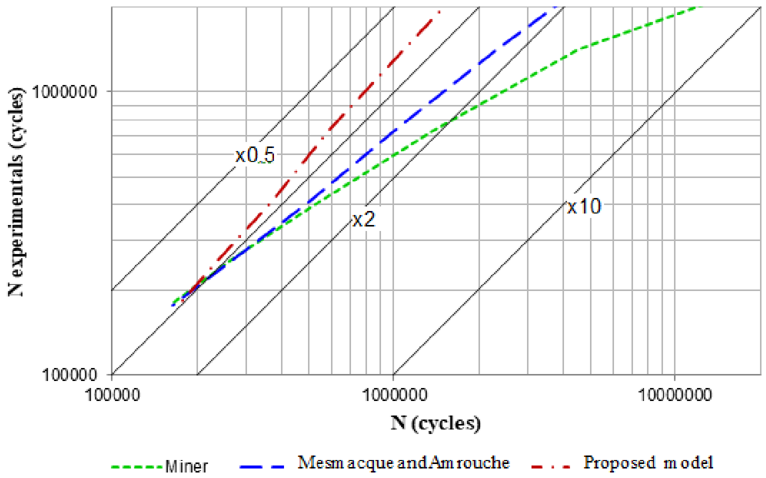


***Figure 13.*** *Material HE 360 D, ratio overload 1.4: experimental lifespans vs lifespans calculated by the three models studied.*

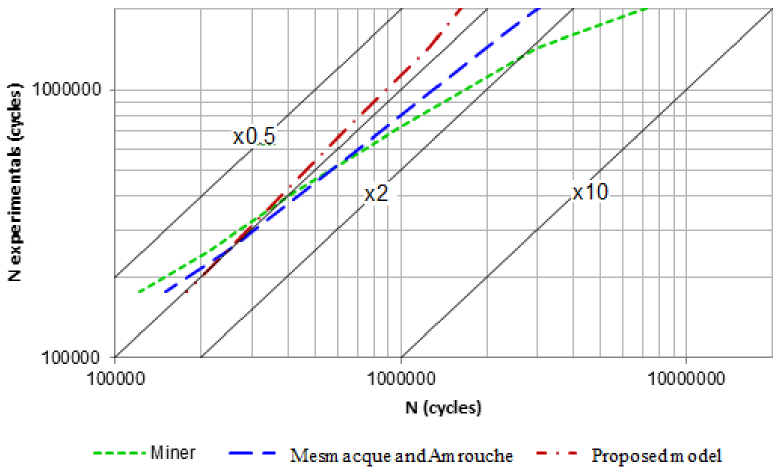


***Figure 14.*** *Material HE 360 Ds, ratio overload 2,3: experimental lifespans vs lifespans calculated by the three models studied.*

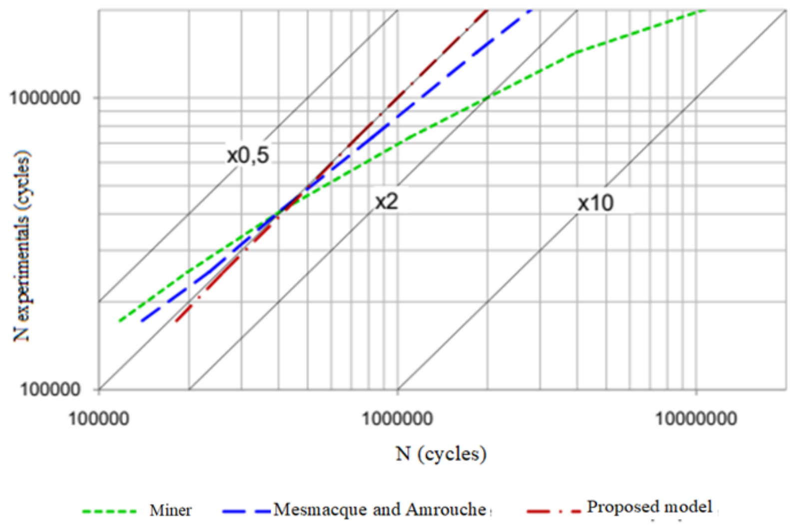


***Figure 15.*** *Material XE 360 D, ratio overload 1, 4: experimental lifespans vs lifespans calculated by the three models studied.*

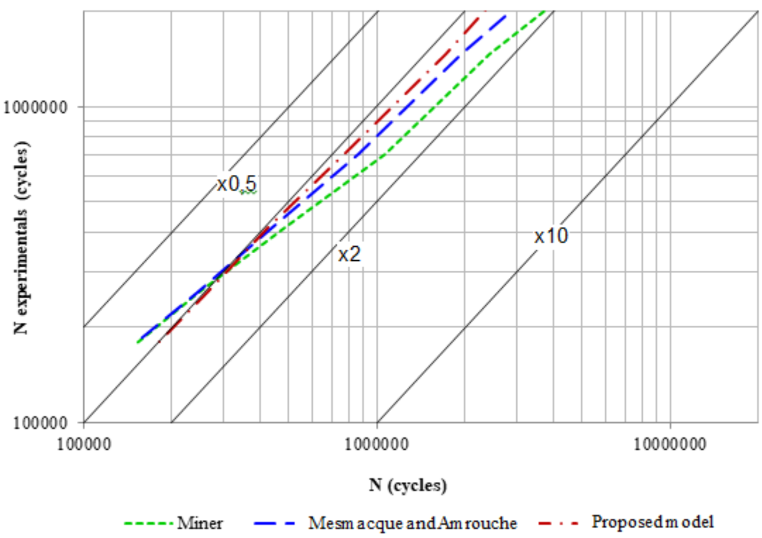


***Figure 16.*** *Material XE 360 D, ratio overload 2,3: experimental lifespans and lifespans calculated by the three models studied.*

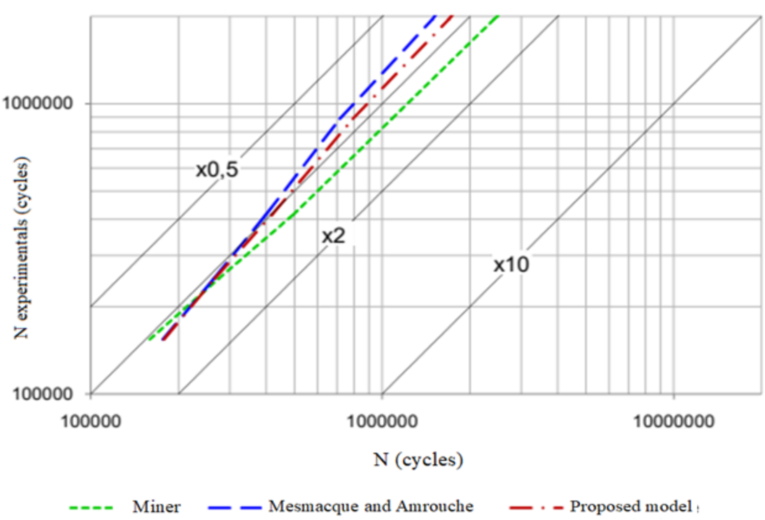


***Figure 17.*** *Material XES 360 D, ratio overload 1, 4: experimental lifespans and lifespans calculated by the three models studied.*

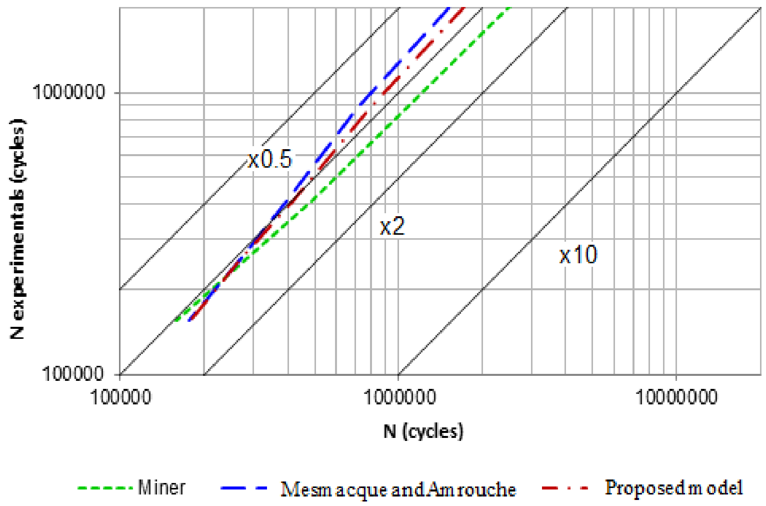


***Figure 18.** Material XES 360 D, ratio overload 2, 3: experimental lifespans and lifespans calculated by the three models studied.*

## 7. Overall Analysis of the Results Obtained

The HE 360 D material appears to be particularly discriminating for the three damage laws used for lifespan calculations, and this for each of the two overload ratios 1.4 and 2.3. Miner's law appears unsuitable because it is highly non-conservative for long lifespans (low effort levels). It also tends to be the most conservative of the three laws used for lifespans of around 2,105 cycles (high stress levels of the experimental F-N curves). The proposed damage model appears conservative and relatively fair in terms of lifespan prediction. The Mesmacque and Amrouche model is rather non-conservative over the entire range of tested lifetimes and is also relatively close to the experimental lifetimes.

The second material, XE 360 D, is discriminating for the overload ratio equal to 1.4. In this case, Miner's law appears unsuitable to describe the fatigue damage of the material both for long lifespans (threshold of unlimited endurance, low effort levels) and for significant loadings (lifetime of the order of $2.10^5$ cycles). The proposed law is the one which best correlates all the experimental results, for each of the two overload ratios. The Mesmacque and Amrouche law also gives good results for predicting the lifespan of this material.

## 8. Conclusion

The presented study highlights the limitations and performances of the different laws for predicting the life of welded points under variable amplitude loading. The tests carried out on three different steels (HE360D, XE360D, XES) revealed two main modes of fatigue failure: sheet metal cracking at medium stresses and shearing of the molten core at high stresses. Among the damage laws analyzed, the Miner law, although simple and widely used, is unsuitable, especially for low loading levels, due to its inability to take into account the interactions between successive load cycles. The Mesmacque and Amrouche law, although more accurate, remains non-conservative at low stresses, thus presenting a certain inadequacy with the experimental results. The proposed damage model, an adaptation of the Chaboche law, stands out for its ability to offer more reliable and consistent predictions. By integrating a specific SN curve calibration approach, this model overcomes the inherent weaknesses of the fluctuating parameters of Chaboche's law. Experimental results confirm that this model provides particularly well-correlated life predictions, even for variable amplitude loadings. In short, the proposed model appears to be the most robust and accurate method for predicting the life of welded points under variable loading, outperforming the other laws studied. These results open promising perspectives for improving prediction methods in design offices, thus contributing to better reliability and safety of welded structures in industrial environments.

The study presented highlights the limitations and performances of the different laws for predicting the lifespan of welded points under loading of variable amplitude. Tests carried out on three distinct steels (HE360D, XE360D, Among the damage laws analyzed, Miner's law, although simple and widely used, proves unsuitable, particularly for low loading levels, due to its inability to take into account the interactions between successive loading cycles. The law of Mesmacque and Amrouche, although more precise, remains non-conservative at low forces, thus presenting a certain inadequacy with the experimental results. The proposed damage model, an adaptation of Chaboche’s law, is distinguished by its ability to provide more reliable and consistent predictions. By integrating a specific calibration approach of the SN curve, this model manages to overcome the weaknesses inherent in the fluctuating parameters of Chaboche’s law. Experimental results confirm that this model provides particularly well-correlated service life predictions, even for variable amplitude loads. In short, the proposed model appears to be the most robust and accurate method for predicting the service life of welded points under variable loading, outperforming the other laws studied. These results open up promising prospects for improving prediction methods in design offices, thus contributing to better reliability and safety of welded structures in industrial environments. A criterion-based approach [12] and the consideration of residual stresses [13] will be a major asset to guarantee the reliability and safety of welded structures.

## Abbreviations

| | |
|---|---|
| D | Damage |
| F-N | Force-Lifespan |
| S-N | Constraint-Lifespan |
| ERP | The Prediction Error |
| $N_R$ | Breaking Life |

## Author Contributions

**Bianzeube Tikri:** Conceptualization, Data curation, Funding acquisition, Investigation, Methodology, Project administration, Resources, Supervision

**Djonglibet Wel-Doret:** Formal Analysis, Validation, Writing – original draft, Writing – review & editing

**Dougabka Dao:** Software, Visualization

## Conflicts of Interest

The authors declare no conflicts of interest.

## References

[1] CHABOCHE J. L. A differential law of fatigue damage with nonlinear accumulation. Revue Française de Mécanique 50-51, 1974.

[2] D. Wel-Doret, Reliable Design of Welded Joints Under Variable Amplitude Loading, Thesis, University of N'Djamena, Chad, 2024.

[3] Nadjitonon, N., Contribution to the modeling of fatigue damage, Doctoral dissertation, Blaise Pascal University, 2010.

[4] ROSSILLON F. Influence des conditions de soudage sur le comportement en fatigue d'un acier THR Dual Phase soudé par point. Thèse de l'Université Blaise Pascal – Clermont II, Clermont-Ferrand, Clermont-Ferrand, 2007.

[5] YOUSEFI F., M. WITT and H. ZENNER, Fatigue strength of welded joints under multiaxial loading: experiments and calculations, Fatigue and Fracture of Engineering Materials and Structures, Vol. 24, pp. 339-355, 2001.

[6] BLONDEAU R. Metallurgy and mechanics of welding, Mechanics and Materials Engineering, Edition Lavoisier, 2001.

[7] B. Tikri, Study of the influence of overloads on the fatigue behavior of spot-welded steels, Thesis, Blaise Pascal University - Clermont-Ferrand, France, 2012.

[8] TIKRI B. Study and improvement of the non-linear damage law of Chaboche, Master 2 Research, Blaise Pascal University - Clermont II, Clermont-Ferrand, 2007.

[9] MESMACQUE G., GARCIA S., AMROUCHE A., RUBIO-GONZALEZ C. Sequential law in multiaxial fatigue, a new damage indicator, International Journal of Fatigue, 2004.

[10] MINER M. A. Cumulative Damage in Fatigue. Journal of Applied Mechanics, September 1945, p. A-159/A-164.

[11] WEBER B. Multiaxial Fatigue of Industrial Structures under Any Load, Thesis of INSA de Lyon, Lyon, 1999.

[12] Boutich O., Belmadi N. E., Etude comparative des critères de fatigue multiaxiale appliquée à des pièces traitées superficiellement. (Mémoire de master, University Abdlhamid Ibn Badis Mostaganem, (2022).

[13] D. Wel-Doret, Influence of residual stresses on the service life of structures under variable amplitude loading, International Journal of Innovation and Applied Studies, 39 (2), pp. 667-675, 2023.